Characterization of the Lanthanide Ion-Binding Properties of Calcineurin-B Using Laser-Induced Luminescence Spectroscopy†

Sarah E. Burroughs‡ and William D. Horrocks, Jr.*

Department of Chemistry, The Pennsylvania State University, University Park, Pennsylvania 16802

Hao Ren and Claude B. Klee

Laboratory of Biochemistry, National Cancer Institute, National Institutes of Health, Bethesda, Maryland 20892

Received April 18, 1994; Revised Manuscript Received June 17, 1994®

ABSTRACT: Calcineurin (CaN) is a Ca^{2+}/calmodulin-dependent protein phosphatase found in brain and other tissues. It is a heterodimer consisting of a catalytic subunit (CaN-A) and a Ca^{2+}-binding regulatory subunit (CaN-B). The primary structure of CaN-B indicates that it, like calmodulin, is an EF-hand protein and binds four Ca^{2+} ions. Eu^{3+}, due to its favorable spectroscopic and chemical properties, has been substituted for Ca^{2+} in CaN-B to determine the metal ion-binding properties of this "calmodulin-like" protein. Excitation of the $^7F_0 \rightarrow {}^5D_0$ transition of Eu^{3+} results in a spectrum similar to that of calmodulin, consisting of three peaks. Analysis of the spectral titration curves reveals four Eu^{3+}-binding sites in CaN-B. The affinities vary: sites I and II have dissociation constants of 1.0 ± 0.2 and 1.6 ± 0.4 μM, respectively; the values for sites III and IV are $K_d = 140 \pm 20$ and $K_d = 20 \pm 10$ nM, respectively. Binding of Tb^{3+} is slightly weaker. Tb^{3+} luminescence, sensitized by tyrosine, reveals that for lanthanides the highest affinity sites lie in the C-terminal domain. Energy transfer distance measurements between Eu^{3+} and Nd^{3+} in sites III and IV reveal a separation of 10.5 ± 0.5 Å, which suggests that these sites are arranged in a typical EF-hand pair. This information indicates that the overall structure of CaN-B is similar to the dumbbell-shaped proteins troponin-C and calmodulin, but is more like TnC in its metal-binding properties.

Calcineurin (CaN)[1] is a Ca^{2+}- and calmodulin (CaM)-binding protein first discovered in brain tissue (Klee & Krinks, 1978; Sharma et al., 1979) and subsequently found in many different tissue types (Klee et al., 1987). It has two subunits: a large "A" subunit (60 kDa) and a small "B" subunit (18 kDa). CaN-A is a class 2B protein phosphatase (Stewart et al., 1982; Winkler et al., 1984), which contains an autoinhibitory region (Hashimoto et al., 1990) as well as separate domains for binding CaM (Kincaid et al., 1988) and CaN-B (Hubbard & Klee, 1989). Calcineurin is a metalloenzyme: CaN-A binds Fe and Zn^{2+} ions (King & Huang, 1984; Rao & Wang, 1989), CaN-B binds four Ca^{2+} ions (Klee et al., 1979), and the phosphatase activity is stimulated by Mn^{2+} (Steward et al., 1982; Winkler et al., 1984; King & Huang, 1984), Ni^{2+} (King & Huang, 1983), and Mg^{2+} ions (King & Huang, 1984; Merat & Cheung, 1993). The recent discovery that CaN binds to immunosuppressive drug–immunophilin complexes (Liu et al., 1991) implicates this enzyme as a central component of the immune response system. Both the A and B subunits are required for CaN binding to such complexes (Ueki et al., 1993), and cross-linking experiments (Li & Handschumacher, 1993) demonstrate that the drug–immunophilin complex binds to the B subunit of holocalcineurin. Furthermore, it has been shown (Fruman et al., 1992) that the activity of CaN, but not other phosphatases, in T-cells is inhibited by drug–immunophilin complexes.

The primary sequence (Table 1) of CaN-B (Aitken et al., 1984; Guerini et al., 1989) shows that it is homologous with CaM (35% identity) and troponin-C (29%). It has a high degree of sequence identity in the Ca^{2+}-binding regions; this homology, as well as its Ca^{2+}-binding properties, classifies CaN-B as an EF-hand protein (Kretsinger, 1973). The subunits do not dissociate in the presence of chelating agents (Klee et al., 1979); however, once dissociated (by urea), Ca^{2+} is required for reassociation (Klee et al., 1985; Merat et al., 1985). The phosphatase activity of the A subunit is highly dependent on its interaction with the B subunit (Merat et al., 1985); in addition, this activity is greatly stimulated by the Ca^{2+}-dependent interaction of CaN with CaM (Stewart et al., 1982). The small subunit, by virtue of its amino-terminal myristoyl group, could allow association of the enzyme with membranes (Towler et al., 1989) or be involved in protein–protein interactions. It has been suggested that the B subunit is involved in the regulation of the enzyme by Ca^{2+} binding, due to the fact that this ion can mildly stimulate the activity of the enzyme even in the absence of CaM (Stewart et al., 1982; Klee et al., 1983). Furthermore, the enzyme's activity is affected by its association with phospholipids (Politino & King, 1987). Elucidation of the metal ion-binding properties of this subunit should shed light on its function.

Eu^{3+} luminescence spectroscopy has a number of advantages in the study of biological systems (Horrocks & Sudnick, 1981; Horrocks, 1993). This technique reveals a wealth of information about the environment of the subject metal ion: characteristics such as ligand charge, number of coordinated water molecules, stoichiometry, binding affinity, and intermetal ion distance can be determined with this method. Its ligand preference and metric similarity to Ca^{2+} make Eu^{3+} an excellent probe for Ca^{2+}-binding sites in proteins. Furthermore, the additional charge on Eu^{3+} often causes higher

† Supported by NIH Grant GM23599 (W.D.H.).

* Author to whom correspondence should be addressed.

‡ Present address: Department of Molecular Genetics and Biochemistry, University of Pittsburgh School of Medicine, Pittsburgh, PA 15261.

® Abstract published in *Advance ACS Abstracts,* August 1, 1994.

[1] Abbreviations: CaN, calcineurin; CaM, calmodulin; TnC, troponin-C; DTT, dithiothreitol; Hepes, *N*-(2-hydroxyethyl)piperazine-*N*′-2-ethanesulfonic acid; Mes, 2-morpholinoethanesulfonic acid; aq, aqueous; equiv, equivalents.

0006-2960/94/0433-10428$04.50/0

Table 1: Amino Acid Sequences of Calcineurin-B, Calmodulin, and Troponin-C

		1	3	5	7	9	12
CaN-B[a]	Myr G N E A S Y P L E M C S H F D A D E I K R L G K R F K K L	D	L	D	N	S	G S L S V E E F M S
CaM[b]	Ac A D Q L T E E Q I A E F K E A F S L F	D	K	D	G	D	G T I T T K E L G T
TnC[c]	D T Q Q A E A R S Y L S E E M I A E F K A A F O M F	D	A	D	G	G	G D I S T K E L G T
CaN-B	L P - E L Q Q N P - - - L V Q R V I D I F	D	T	D	G	N	G E V D F K E F I E G V S Q F S V K
CaM	V M R S L G Q N P T E A E L Q D M I N E V	D	A	D	G	N	G T I D F P E F L T M M A R K M K D
TnC	V M R M L G Q T P T K E E L D A I I E E V	D	E	D	G	S	G T I D F E E F L V M M V R Q M K E D A K
CaN-B	G D K E Q K L R F A F R I Y	D	M	D	K	D	G Y I S N G E L F Q V L K M M V G N N L K D T Q L
CaM	T D S E E E I R E A F R V F	D	K	D	G	N	G Y I S A A E L R H V M T - - - - - N L G E K L T
TnC	G K S E E E L A E C F R I F	D	R	N	A	D	G Y I D A E E L A E I P R - - - - - A S G E H V T
CaN-B	Q Q I V D K T I I N A	D	K	D	G	D	G R I S F E E F C A V V G G S L D I H K K M V V D D
CaM	D E E V D E M I R E A	D	I	D	G	D	G Q V N Y E E F V Q M M T A K
TnC	D E I E E S L M K A G	D	K	N	N	D	G R I D F D E F L K M M E G V Q

[a] Aitken et al., 1984. [b] Bovine uterine. Grand & Perry, 1978. [c] Rabbit skeletal. Collins, 1974.

affinity and spontaneous replacement of the native Ca^{2+}. Another difference between these two ions is coordination number: Ca^{2+} will accommodate seven or eight ligands, whereas Eu^{3+} prefers eight or nine.

Tb^{3+} luminescence, although lacking some of the benefits of Eu^{3+}, is useful when this ion serves as an energy acceptor for intrinsic fluorophores such as phenylalanine, tyrosine, or tryptophan. This phenomenon, termed sensitized emission, has been observed in many proteins (Brittain et al., 1976). This technique allows one to probe lanthanide-binding sites in the vicinity of an intrinsic fluorophore, thereby providing information about a specific region of a protein. Lanthanide luminescence has been used to characterize Ca^{2+}-binding proteins such as calmodulin (Mulqueen et al., 1985; Horrocks & Tingey, 1988; Bruno et al., 1992) and troponin-C (Wang et al., 1981, 1982), as well as other metal ion-binding proteins (Eads et al., 1985; Snyder et al., 1981).

In this paper, luminescence studies of Eu^{3+} and Tb^{3+} binding to CaN-B are described. Information regarding stoichiometry and binding affinity is compared to findings for the homologous proteins CaM and TnC to assess their functional similarities. The effect of Mg^{2+} on lanthanide ion binding to the subunit and protein conformation, as evidenced by competition studies and luminescence changes, is also reported.

MATERIALS AND METHODS

Molecular Cloning and Construction of the CaN-B Expression Vector. Restriction enzyme digestions and ligations, DNA gel electrophoresis, and other recombinant DNA techniques were performed essentially as described by Sambrook et al. (1989). The human calcineurin-B-coding region (Guerini et al., 1989) was transferred to the pOTSN*co*I2 vector (Shatzman & Rosenberg, 1987) to generate plasmid pASCnB (D. Guerini, unpublished). As part of this reconstruction, an *Nco*I site was introduced at the initiator codon to facilitate transfer to other vectors. The *Nco*I–*Bst*YI DNA fragment excised from plasmid pAS-CnB, carrying the entire coding sequence of calcineurin-B and the termination codon, was subcloned into the expression vector pET3d (Novagen, Madison, WI) under the control of the T7 RNA polymerase promoter (Studier et al., 1990) to generate plasmid pBE.

Expression and Purification of Calcineurin-B. Escherichia coli strain BL21 (DE3) plyS (Novagen), a DE3 lysogen containing the T7 RNA polymerase gene under the *Lac* UV5 promoter, was transformed with pBE and grown at 37 °C in LB medium containing 100 mg/L ampicillin and 30 mg/L chloramphenicol. When the absorbance at 600 nm reached 0.7, the production of protein was induced by the addition of isopropyl β-D-thiogalactoside to a final concentration of 1 mM. After 5 h, the cells were harvested by centrifugation, washed, and stored at −70 °C. The frozen cells were processed in batches of 2.5 L, and CaN-B was purified as described (Anglister, 1994). The purified protein was stored at −70 °C in DTT under N_2 to prevent disulfide cross-linking. It should be noted that this protein does not contain the amino-terminal myristoyl blocking group found in the native subunit (Aitken et al., 1982). The sample required a final purification step in order to remove a high molecular weight contaminant and to exchange the protein into a buffer containing 40 mM Hepes (pH 7.0) (Sigma), 0.5 M KCl (Fisher), and 0.4 mM DTT (Boehringer Mannheim). This was accomplished on a Waters 600E HPLC with a Phenomenex GP200 size exclusion column (25 × 1.0 cm, 10-μm pore size) at 4 °C. Approximately 100 μL of a 6 mg/mL stock solution was chromatographed at 2 mL/min buffer. The fractions were collected and their UV spectra checked for the characteristic fine structure of CaN-B. The CaN-B-containing fractions were concentrated using an Amicon 8010 stirred ultrafiltration cell (Amicon/W. R. Grace) with a YM10 membrane at 50 psi. The concentrated protein was stored at −20 °C. Protein concentration was determined by BCA assay (Pierce) using a CaM standard.[2] The molar absorptivity of nonmyristoylated CaN-B, ϵ_{276}, is 4650 M^{-1} cm^{-1}. For luminescence experiments where a lower pH was required, 40 mM Mes (Sigma) at pH 6.0 was used in lieu of Hepes buffer.

Luminescence Experiments. Lanthanide salt and buffer solutions were made in either Nanopure H_2O (Barnstead) or

[2] The use of CaM as a standard in this assay is justified by the fact that the reactivity of a protein in this assay is dependent on the protein's macromolecular structure, the number of peptide bonds, and the cysteine, tryptophan, and tyrosine content. These characteristics are very similar in CaM and CaN-B.

99.9% D_2O (Aldrich). Metal ion concentrations were determined by chelometric titration (Fritz et al., 1958) with standardized EDTA (Fisher) using an arsenazo indicator.

Eu^{3+} luminescence spectroscopy experiments were performed using a Continuum (formerly Quantel) TDL50 Nd:YAG laser-pumped tunable dye laser, which provides a 70–90-mJ pulse at 10 Hz. The $^7F_0 \rightarrow {}^5D_0$ transition wavelength (577–582 nm) was accessed using a mixture of rhodamine 590 and 610 dyes (Kodak). Emission ($^5D_0 \rightarrow {}^7F_2$) was monitored at 614 nm with a Hamamatsu photomultiplier tube and recorded via a LeCroy interface to a Swan 386SX computer. Samples were held in a quartz semi-microcuvette (Uvonic) and stirred gently.

Generally, 0.4 mL of a 5 μM protein sample was titrated with Eu^{3+}, and either the excitation spectrum or the emission decay was recorded at each point. Measurement of the dissociation constants for the tighter binding sites was achieved by low-concentration titrations, where 0.4 mL of a 0.2 μM protein solution in D_2O buffer was titrated with Eu^{3+}. Total emission intensity was collected during excitation at a single specific wavelength (as opposed to a spectral scan). All lanthanide ion-binding experiments were conducted at a temperature of approximately 10 °C to minimize solvent evaporation and sample denaturation.

Spectra were resolved into Gaussian–Lorentzian peaks (McNemar & Horrocks, 1989) and luminescence decays into their component exponentials, yielding amplitudes I_0 and lifetimes τ for each of the components, using the computer program PeakFit (Jandel Scientific). Metal ion–ligand equilibrium binding curves were analyzed using EQUIL (Goldstein & Leung, 1990), a computer program that determines dissociation constants based on a user-defined model and intensity vs concentration data.

Tb^{3+} luminescence was measured on a SPEX Fluorolog 2 spectrofluorometer equipped with a phosphorimeter, with excitation at either 225 (direct excitation of Tb^{3+}) or 278 nm (luminescence of Tb^{3+} sensitized by tyrosine); emission was monitored at 543 nm. A Schott 515-nm cut-on filter was used in the emission beam to eliminate scattered light and noise. Emission photon flux (counts per second) as a function of Tb^{3+} concentration was measured on 0.5-mL 0.2–20 μM CaN-B samples, buffered as above, with up to 6 equiv of Tb^{3+} added. Due to the sensitivity of fluorescence intensity to temperature observed with this instrument, it was necessary to allow samples to equilibrate to the instrument cell holder temperature (9–10 °C). A continuous wave, 450-W xenon lamp was used for measurements of total intensity, whereas a pulsed 150-W lamp was the excitation source for lifetime measurements.

Energy transfer experiments were conducted on various H_2O/D_2O mixtures by the addition of 0.5–0.8 equiv of donor metal ion (Eu^{3+}) to a 1–5 μM protein solution, followed by the addition of 0.5–1.5 equiv of acceptor metal ion (Nd^{3+}); excited-state lifetimes were measured at each point to calculate the efficiency of energy transfer. No more than 2 equiv of total Ln^{3+} was added in order to avoid filling the weak-binding sites.

RESULTS AND DISCUSSION

Eu^{3+} Luminescence: Stoichiometry and Affinities of Eu^{3+} in CaN-B. Examination of the primary structure of CaN-B reveals four EF-hand sequences similar to those found in the dumbbell-shaped proteins TnC and CaM. These four EF hands are known to be Ca^{2+}-binding sites (Aitken et al., 1984) and therefore have the potential to bind lanthanide ions. The first goal was to determine whether and how many of these Ca^{2+}-binding sites actually bind Eu^{3+}. The $^7F_0 \rightarrow {}^5D_0$ luminescence excitation spectrum of Eu^{3+} in the protein (Figure 1) can be resolved into three peaks, with maxima at 579.26, 579.46, and 579.64 nm. This spectrum is somewhat different from that observed for Eu^{3+} in CaM (Bruno et al., 1992), where the spectrum is resolved into peaks of 579.21, 579.31, and 579.58 nm. The wavelength of the middle peak is 0.15 nm lower in CaM than in CaN-B, suggesting a difference in ligand environment for the site corresponding to this peak. Another difference between the spectra of the two proteins is the relative intensities of the peaks; the intensity of the lowest wavelength peak, relative to the middle peak, is much higher in CaM than in CaN-B. At pH 6.0, with 4.0 equiv of Eu^{3+} in CaN-B, the intensities of the two peaks are about equal. However, in the presence of 1 mM Mg^{2+}, the 579.24-nm peak reaches a maximum intensity of about twice that of the 579.46-nm peak; this spectrum more closely resembles that of CaM.

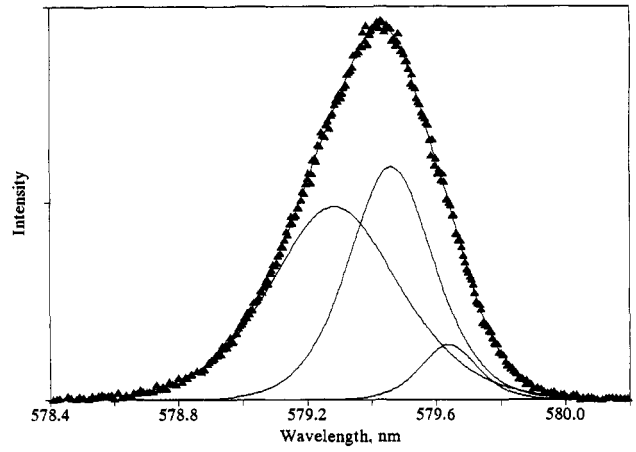

FIGURE 1: Excitation spectrum of 2.5 equiv of Eu^{3+} in 5.0 μM CaN-B at pH 7.0. The spectrum has been resolved into three peaks with maxima at 579.24 (fwhm = 0.48 nm), 579.46 (0.31 nm), and 579.64 nm (0.21 nm).

Although the wavelengths differ somewhat, the full width at half-maximum (fwhm) values of the resolved peaks of CaN-B (0.46, 0.31, and 0.21 nm) are strikingly similar to those obtained by Bruno et al. (1992) for CaM (0.50, 0.27, and 0.22 nm). These features suggest that the overall metal ion-binding environment of CaN-B is comparable to that of CaM. Additionally, the Eu^{3+} luminescence excitation spectrum of parvalbumin (McNemar & Horrocks, 1990), another typical EF-hand protein, displays peak widths (0.49 and 0.32 nm for the Carp III isotype) much the same as those of CaN-B.

The variations in peak intensities and wavelengths are probably due to minor conformational differences between the two proteins. The presence of only three resolvable peaks in the excitation spectrum does not preclude the existence of four Eu^{3+}-binding sites in the protein; indeed, the spectrum of CaM (Bruno et al., 1992), which has four known Eu^{3+}-binding sites, is also resolvable into only three peaks. This merely indicates that the characteristics of the sites are too much alike to be resolved spectrally.

A plot of the resolved peak intensities as a function of Eu^{3+} concentration added to CaN-B is shown in Figure 2. Initial curve-fitting based on a three-site, one site per peak model produced a poor fit (data not shown). After careful analysis of the fits to several models, it became apparent that the tight site gives rise to two peaks in the spectrum, one of which is at the same wavelength as the peak attributable to another

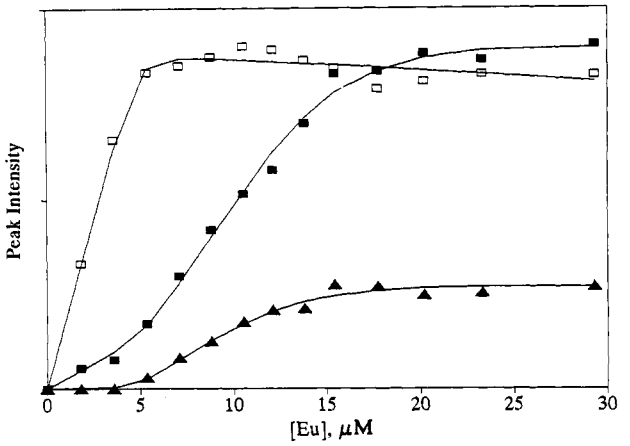

FIGURE 2: Plot of peak intensity vs Eu^{3+} concentration for a titration of this metal ion into 5.0 μM CaN-B at pH 6.0: ■, 579.24 nm; □, 579.46 nm; ▲, 579.64 nm. The lines drawn through the data represent the best fit based on a four-site model where the 579.24-nm peak is a composite of three peaks, one of which is due to the same site as that giving rise to the 579.46-nm peak.

site. The $^7F_0 \rightarrow {}^5D_0$ transition of Eu^{3+} is nondegenerate, producing only one excitation peak for each unique environment; therefore, the appearance of two peaks for one species indicates that two similar, but nonidentical, environments exist (although the environments may be different conformations of the same complex). Although unusual for biological systems, this phenomenon has been observed in parvalbumin (McNemar & Horrocks, 1990; Henzl et al., 1985) where, at certain pH values, two peaks corresponding to the same binding site are observed. Since the titration curve corresponding to the intensity of the 579.46-nm peak is quantitative to 1 equiv, any other peaks appearing before this peak reaches maximum intensity *must* be due to the same site; conversely, if there were two independent sites binding with equal affinities, the curve corresponding to the peak at 579.46 nm would break at 2 equiv of Eu^{3+} instead of at 1 equiv. The best fit of the data, as judged by graphical inspection and statistical analysis (χ^2 values), indicates a stoichiometry of four Eu^{3+} ions per CaN-B molecule. The peak centered at 579.26 nm is actually a composite of intensity contributions from Eu^{3+} in three sites, of which one site is the same as that giving rise to the peak at 579.46 nm. This model, although rather complex, gives the best fit to the data and provides a reasonable description of the binding of Eu^{3+} to CaN-B. This is best illustrated by comparing the fits of the titration of Eu^{3+} into CaN-B in the presence of 1 mM Mg^{2+}, as shown in Figure 3. Evaluation of the fits of the data to several models demonstrates that the four-site model (c) gives the best fit, especially for the 579.64-nm data. The χ^2 values calculated for these fits also indicate that the four-site model is best.

Comparison of the Eu^{3+} titration data sets in the absence and presence of Mg^{2+} reveals a small degree of competition between these two metal ions. A dissociation constant of about 0.4 mM for Mg^{2+}CaN-B is calculated by the simultaneous fitting of data to a four-site Mg^{2+}- and Eu^{3+}-binding model. Relative peak intensities were also changed upon the addition of Mg^{2+}; the luminescence intensity of the 579.26-nm peak is greatly enhanced in the presence of this metal ion.

Because the spectrum observed for Eu^{3+} in parvalbumin is pH dependent, an attempt was made to simplify the spectrum of CaN-B by changing the pH of the protein solution (that is, it was hoped that the component of the 579.24-nm peak due to the same site as the 579.45-nm peak could be eliminated). When the protein is put into Mes buffer at pH

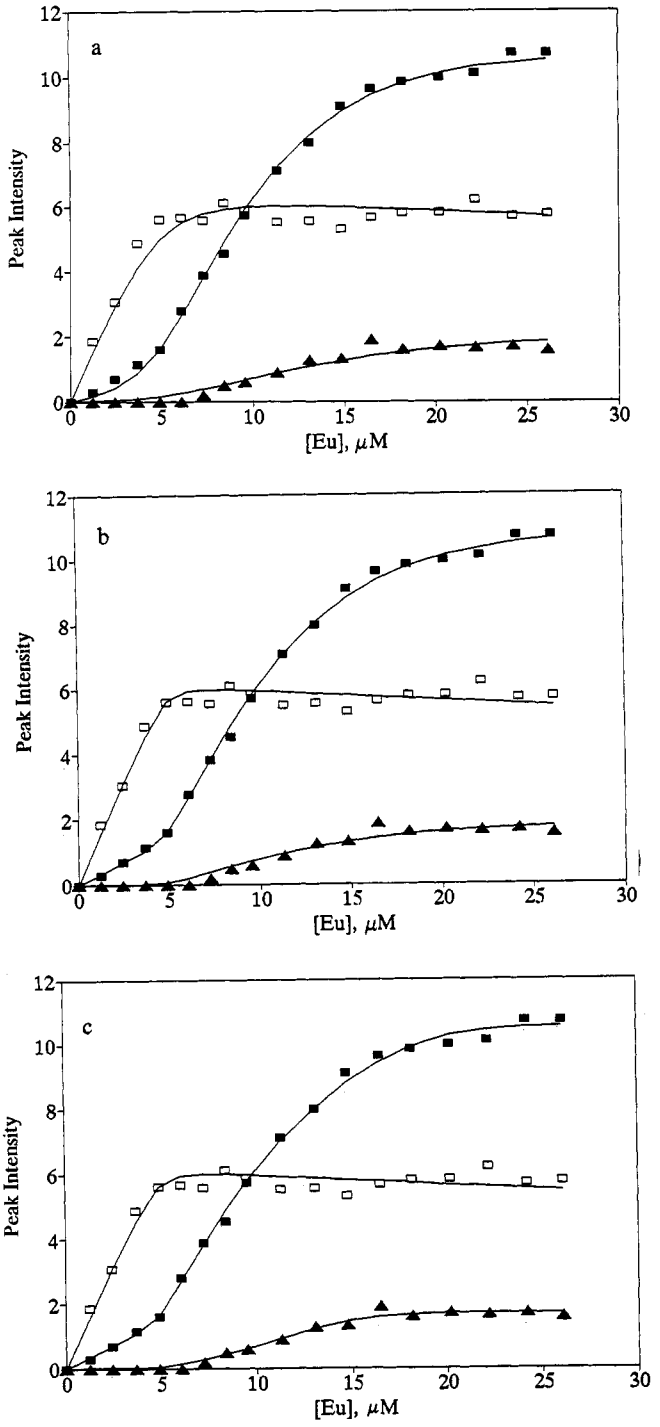

FIGURE 3: Plot of peak intensities as a function of Eu^{3+} concentration for a titration of this metal ion into 5.0 μM CaN-B in 40 mM Mes (pH 6.0), 0.5 M KCl, 0.4 mM DTT, and 1 mM Mg^{2+}: ■, 579.24 nm; □, 579.46 nm; ▲, 579.64 nm. The lines drawn through the data represent the various fits of the spectral titration data: (a) three-site, one peak per site model (χ^2 = 90); (b) three-site model where the peak at 579.24 nm is a composite of two peaks, one of which is due to the same site as that giving rise to the 579.46-nm peak (χ^2 = 61); (c) four-site model where the 579.24-nm peak is a composite of three peaks, one of which is due to the same site as that giving rise to the peak at 579.46 nm (χ^2 = 49).

6.0, spectral changes do occur; although the component of the 579.24-nm peak arising first is not removed, its intensity is diminished. At the beginning of the titration (before 1.0 equiv of Eu^{3+} has been added) the ratios of peak intensities ($I_{579.45}/I_{579.24}$) are approximately 3 at pH 7.0 and 7 at pH 6.0. This is fortunate because this variation in peak intensity at pH 6.0

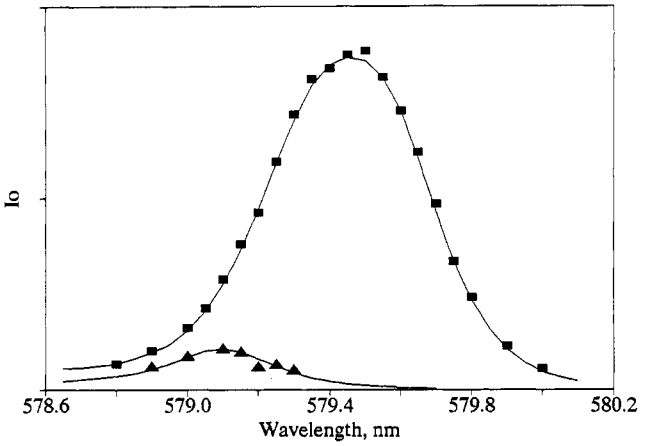

FIGURE 4: Time-resolved spectrum of 3.0 equiv of Eu^{3+} in 5 μM CaN-B at pH 7.0. Intensities at time zero (I_0) of the 0.28-ms (▲) and 0.52-ms (■) lifetimes are plotted as a function of excitation wavelength.

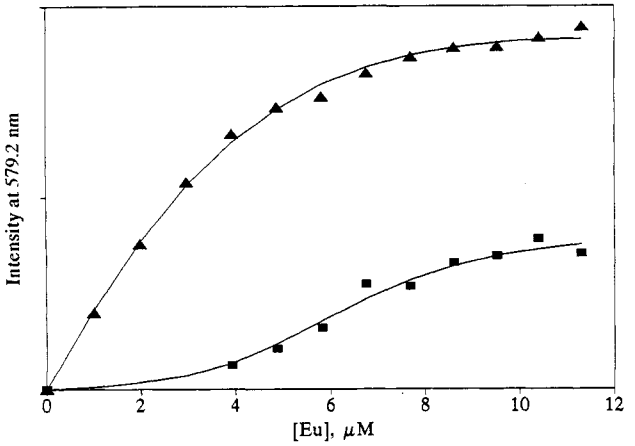

FIGURE 5: Lifetime-monitored titration of Eu^{3+} into 2 μM CaN-B at pH 7.0. I_0 values of the 0.52-ms (▲) and 0.28-ms (■) lifetimes, resulting from excitation of the sample at 579.2 nm, are plotted as a function of Eu^{3+} concentration. The data are fit to a four-site model, where the 0.52-ms intensity is due to three sites and the 0.28-ms intensity corresponds to one site.

results in a clear break in the 579.24-nm data, which allows the curve to be resolved by EQUIL into three components.

Eu^{3+} Luminescence Decay Constants: Number of Coordinated Water Molecules and Further Resolution of the 579.24-nm Peak. Additional information about the environment of Eu^{3+} can be obtained by recording the time course of luminescence decay separately in H_2O and D_2O solutions. It has been shown by Horrocks and Sudnick (1979) that the number of water molecules, q, in the first coordination sphere of Eu^{3+} is given by

$$q = 1.05(\tau_{H_2O}^{-1} - \tau_{D_2O}^{-1}) \quad (1)$$

where τ^{-1} is the reciprocal of the excited-state lifetime (ms^{-1}) in the solvent indicated. The difference in observed deexcitation rates (τ values) among Eu^{3+}-binding sites in CaN-B is not as great as in CaM. In H_2O solution, two lifetimes (0.52 and 0.28 ms) are observed for CaN-B; two lifetimes are also observed in CaM. However, in D_2O three lifetimes are found in CaM, whereas only a single exponential decay is seen in CaN-B (τ_{D_2O} = 2.13 ms). By use of eq 1, the numbers of inner-sphere-coordinated water molecules are calculated to be 3.2 ± 0.5 for τ_{H_2O} = 0.28 ms and 1.5 ± 0.5 for τ_{H_2O} = 0.52 ms; the latter value most likely represents an average value for the sites whose separate lifetimes cannot be resolved.

In order to find out where in the excitation spectrum the different lifetimes contribute, a time-resolved spectrum was recorded. In this type of experiment, luminescence decays are recorded at 0.1- or 0.05-nm increments along the excitation spectrum. The amplitudes of the component expoentials, I_0, are plotted as a function of excitation wavelength to produce a spectrum such as the one shown in Figure 4. The 0.28-ms peak is centered at about 579.1 nm, although the spectrum is dominated by the 0.52-ms-lifetime component. The 0.28-ms peak thus is probably due to one of the sites giving rise to the excitation spectral peak at 579.24 nm, which cannot be resolved in the energy (wavelength) domain.

By recording the luminescence decay during a titration of CaN-B with Eu^{3+}, resolving it into component exponential functions, and plotting the resultant I_0 values, the curve shown in Figure 5 was obtained. From this experiment, it is apparent that the site with τ = 0.28 ms corresponds to a weak-binding site. This curve provides independent binding data for one of the three components of the 579.24-nm peak, complementing the spectral titration data. By the combination of spectral and lifetime data, a description of the binding of Eu^{3+} to each site is achievable.

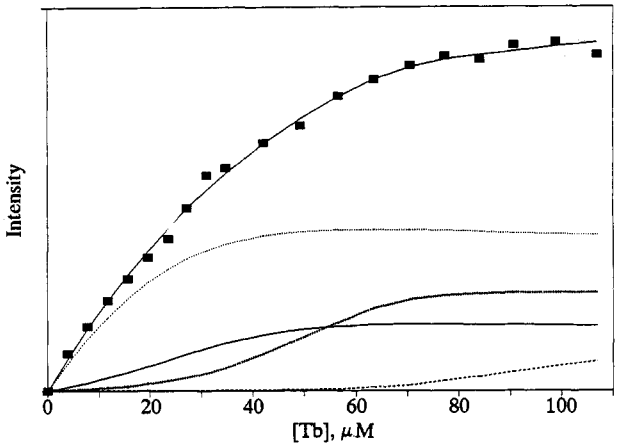

FIGURE 6: Titration of Tb^{3+} into 18 μM CaN-B in 40 mM Hepes (pH 7.0), 0.5 M KCl, and 0.4 mM DTT. Emission intensity at 543 nm is caused by direct excitation of Tb^{3+} at 225 nm. The line drawn through the data is the best fit to a four-site model, including the known intensity contribution from Tb^{3+}(aq) (- - -). These data yield dissociation constants of 40 nM (—), 170 nM (• • •), and two sites at 1.3 μM (•••).

Tb^{3+} Luminescence: Sequence of Lanthanide Ion Binding in Calcineurin-B. Tb^{3+} luminescence titrations were performed to determine the stoichiometry (by direct excitation) and sequence of binding (by tyrosine-sensitized luminescence). Titration of Tb^{3+} into 18 μM CaN-B, monitored by direct excitation at 225 nm, results in the curve shown in Figure 6; the curve drawn through the data is the best-fit curve based on a four-site model, which includes an intensity contribution from free Tb^{3+}(aq). The inclusion of the free Tb^{3+}(aq) intensity in the model is necessary for two reasons: (1) Tb^{3+} is not as severely quenched by H_2O as Eu^{3+} luminescence is, which gives it appreciable intensity at this concentration, and (2) an ordinary fluorometer does not permit the fine wavelength resolution required to avoid the excitation of the Tb^{3+}(aq) ion. The Tb^{3+}(aq) intensity parameter was calculated by measuring the emission intensity of Tb^{3+} in the experimental buffer; this value was held constant in the EQUIL calculations. The three-site model did not give a good fit (data not shown), confirming the presence of four lanthanide ion-binding sites in CaN-B. The dissociation constants for the two tighter sites,

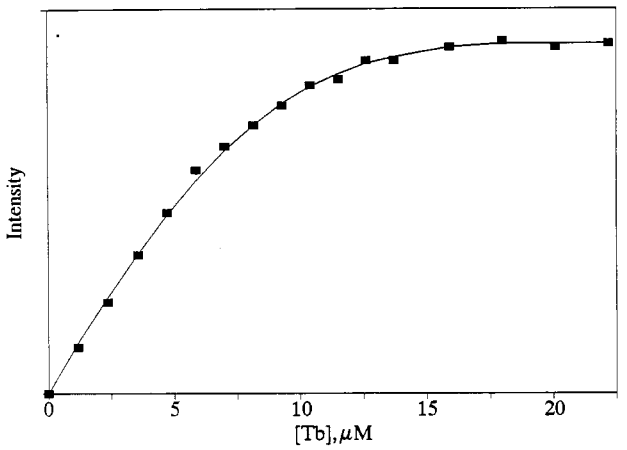

FIGURE 7: Titration of Tb^{3+} into 5.0 μM CaN-B at pH 7.0. Sensitized emission of Tb^{3+} at 543 nm is caused by excitation at 278 nm. The line drawn through the data represents the best fit based on a four-site model with intensity contribution from two sites (χ^2 = 10.6).

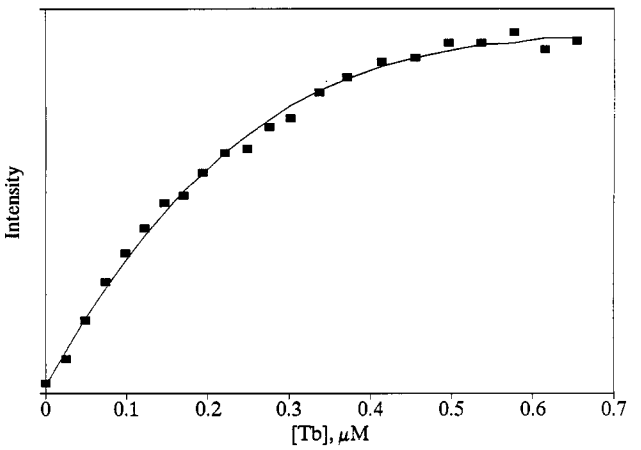

FIGURE 8: Titration of Tb^{3+} into 200 nM CaN-B at pH 7.0, monitored by sensitized emission. The line drawn through the data represents the best fit based on a four-site model with intensity contributions from two sites. Combination of these data with those acquired at 5.0 and 18 μM yields K_d values of 40 ● 10 nM, 170 ± 20 nM, and 1–3 μM.

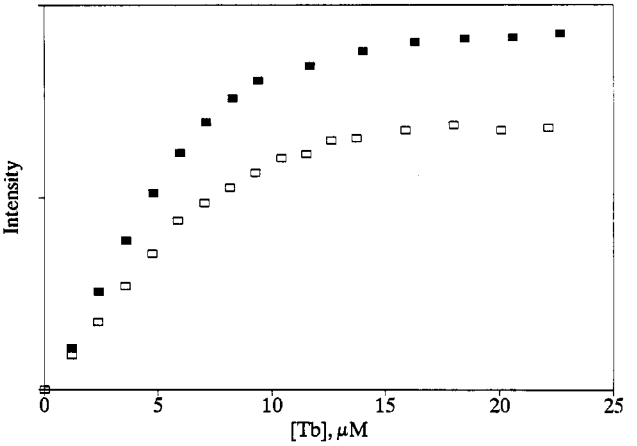

FIGURE 9: Titration of Tb^{3+} into 5.0 μM CaN-B at pH 7.0 in the presence (■) and absence (□) of 1 mM Mg^{2+}. Sensitized emission of Tb^{3+} at 543 nm is caused by excitation at 278 nm.

which bind nearly quantitatively in this experiment, cannot be measured via experiments carried out at this concentration; the resolved curves in Figure 6 were produced by simultaneous fitting of this data, in EQUIL, with data from a sensitized emission experiment done at 0.2 μM (see Figure 8) in order to measure these higher binding affinities.

Sensitized emission has been observed in many proteins (Brittain et al., 1976). The inverse sixth power distance dependence of this phenomenon is particularly useful when deducing proximity relationships between intrinsic fluorophores and the metal ion-binding site. Thus, the conserved tyrosine residue in position 7 of the loop in site III (the third EF-hand sequence from the C-terminus) in dumbbell-shaped proteins (see Table 1) is expected to strongly sensitize luminescence from Tb^{3+} in this site. This advantageous situation has been exploited to determine the order of lanthanide ion binding in CaM (Mulqueen et al., 1985; Kilhoffer et al., 1980; Wang et al., 1984) and TnC (Leavis et al., 1980). The determination of the Tb^{3+} ion-binding sequence is possible in CaN-B due to the existence of the conserved tyrosine residue (Tyr105) in the site III loop, as well as an additional tyrosine (Tyr98) in the helix preceding the site III loop. The sensitized Tb^{3+} emission measured in a titration of 5 μM CaN-B with Tb^{3+} is shown in Figure 7. These data are well fit by a model where the two highest affinity sites are sensitized (a one-site model does not fit well to the data). Thus, we find that Tb^{3+} binds to sites III and IV first, followed by binding to sites I and II. This analysis requires, and it was found, that no Tb^{3+} emission is observed for a third or fourth site, indicating that the sites in the N-terminal lobe of the protein are not sensitized by tyrosine. The tyrosine residue near the amino terminus (Tyr6) apparently does not sensitize Tb^{3+} bound in this lobe of the protein, suggesting that it is fairly far away from the metal ion-binding loops. NMR structural data (Anglister et al., 1994) indicate that this region is highly flexible, so that it may have an extended conformation.

In order to determine the dissociation constants of Tb^{3+} in sites III and IV, a titration of this metal ion into 200 nM CaN-B was monitored by sensitized luminescence (Figure 8). Combination of this data set with those acquired at 18 and 5 μM yield the following K_d values. For the carboxyl-terminal sites, Tb^{3+} K_d's are 40 ± 10 and 170 ± 20 nM at pH 7.0; the two amino-terminal sites have K_d's for Tb^{3+} of 1–3 μM.

In the presence of 1 mM Mg^{2+}, the luminescence intensity of Tb^{3+} in CaN-B is enhanced. The enhanced emission may be due to a conformational change that the protein undergoes when exposed to Mg^{2+} [as evidenced by the UV difference spectrum (Klee et al., 1987)], which creates a more luminescent species. Although possible, it is unlikely that a Mg^{2+}-induced change in the relative orientation of the tyrosine with respect to the Tb^{3+} (resulting in greater sensitization) is responsible for this effect because the same result is observed in the Eu^{3+} spectrum. A more plausible explanation is that the conformational change results in a change in site symmetry that may make the transition more allowed, thus increasing the radiative rate constant. A sensitized emission-monitored titration of Tb^{3+} into 5 μM CaN-B containing 1 mM Mg^{2+} is shown in Figure 9, with the Mg^{2+}-free data displayed for comparison. In addition to being more luminescent, in the presence of Mg^{2+} the Tb^{3+} ion is bound with slightly lower affinity. Analysis of the Tb^{3+}CaN-B binding curves with and without Mg^{2+}, using the EQUIL program, indicates an average affinity of Mg^{2+} for the four sites of CaN-B of 0.4 mM.

The lanthanide ion-binding behavior in CaN-B is very similar to that observed in rabbit skeletal TnC (Leavis et al., 1980), where the Tb^{3+} binds to sites III and IV and is sensitized by Tyr109. However, this result is different from that in CaM (Kilhoffer et al., 1980), where the first two metal ions to bind are very weakly sensitized by tyrosine and the second

two equivalents are highly sensitized. These data suggest that the order of lanthanide ion binding (sites III and IV before sites I and II) is the same as that of troponin-C, but opposite from that of calmodulin. Closer inspection of the amino acid sequences in the Ca^{2+}-binding loops in these proteins (Table 1) reveals an interesting pattern. In a review of Ca^{2+}-binding proteins, Marsden, Shaw, and Sykes (Marsden et al., 1990) compared Ca^{2+}-binding loops from the TnC superfamily and found that although the residue at position 9 in the loop usually does not directly coordinate the metal ion, it may be important in determining Ca^{2+} affinity. Looking at the coordinating residues (positions 1, 3, 5, 7, 9, and 12), as determined by the crystal structure of Ca^{2+}CaM (Babu et al., 1988), it is interesting to note that the number of carboxylate residues in these positions in the four binding loops is exactly the same for CaN-B and TnC (3, 4, 4, 4), but different for CaM (4, 4, 3, 4). The higher total ligand charge in the carboxyl-terminal lobes of CaN-B and TnC may induce binding to this lobe first. Furthermore, the lobe of the molecule with more carboxylates in one loop binds *both* lanthanide ions first; this suggests an element of cooperativity, which has been observed in Ca^{2+} binding to troponin-C (Jahnke & Heilmeyer, 1980) and calmodulin (Minowa & Yagi, 1984).

The question of which of the two tight-binding sites, III or IV, binds first in CaN-B may be answered by looking at the crystal structure of troponin-C (Herzberg & James, 1988). Position 7 of the site III loop is highly conserved among EF-hand proteins: this position is nearly always occupied by a tyrosine or phenylalanine residue. Although this residue is in site III, the close association of sites III and IV places this residue in close proximity to the metal ions occupying both of these sites. Turkey skeletal muscle troponin-C, which is highly homologous to CaN-B in the EF-hand-pair region, possesses a phenylalanine residue (Phe105) in the helix preceding the third loop, a position analogous to the Tyr98 of CaN-B. The distances between Phe105 and the Ca^{2+} ions in sites III and IV differ by about 5 Å, whereas Phe112 (position 7 of the loop) lies roughly equidistant from the two metal ions in this crystal structure. Although no assumptions can be made about the orientations of the chromophoric residues in CaN-B (and their effect on efficiency), on the basis of the distance dependence of energy transfer efficiency, chances are that site III, with its two tyrosine residues close by, is more strongly sensitized than site IV. Thus, a tentative assignment of site III as the tightest Ln^{3+}-binding site of CaN-B can be made.

Assignment of Peaks in the Eu^{3+} Spectrum of Calcineurin-B. The combination of Tb^{3+} and Eu^{3+} data allows the assignment of the peaks in the Eu^{3+} excitation spectrum to Ca^{2+}-binding sites in the protein. Because the 579.46-nm peak in the Eu^{3+} spectrum (Figure 1) exhibits quantitative binding and the Tb^{3+} sensitized emission experiments suggest that site III binds first, the Eu^{3+} CaN-B peak at 579.46 nm is assigned to site III and the component of the 579.24-nm peak arising second to site IV. The relationship between total ligand charge and transition frequency described by Albin and Horrocks (1985) can be used as a guide to assign the spectral peaks to particular sites in the protein. By comparison of the environments of sites I and II, it may be deduced that site I, with three carboxylates in the coordinating positions, gives rise to the peak at 579.24 nm and that the peak at 579.64 nm is due to site II, which contains four carboxylate residues in the loop.

From these peak assignments, it follows that the shorter luminescence lifetime arises from Eu^{3+} in site I (Figure 4); the spectral data (i.e., Figure 3) provide individual binding data for sites III and II. By combination of these experiments in EQUIL, it is possible to calculate the K_d's for Eu^{3+} in the binding sites of CaN-B. Sites I and II are determined to bind with K_d's of 1.0 ± 0.2 and 1.6 ± 0.4 μM, respectively. Site IV has $K_d = 140 \pm 20$ nM, and the dissociation constant of site III is calculated to be 20 ± 10 nM. The large estimated error for the latter measurement is due to the fact that the experiments were necessarily done at a concentration 2 orders of magnitude above the calculated K_d, which prevents an accurate measurement of the affinity. However, the Tb^{3+} data taken at 200 nM give a K_d value of 40 nM, which is similar to the Eu^{3+} value. Eu^{3+} typically displays slightly tighter binding to Ca^{2+}-binding sites than does Tb^{3+}, probably due to the size difference between these two ions and the preference of Ca^{2+}-binding sites [Ca^{2+} ionic radius, 1.20 Å (Shannon, 1976)] for the metrically similar Eu^{3+} (1.21 Å) over Tb^{3+} (1.18 Å). Furthermore, the difference in hydration energies between the two lanthanides may contribute to the difference in their affinities.

Although the small subunit used in these experiments is a nonmyristoylated recombinant protein, it is reasonable to assume that these studies are directly applicable to the native (that is, myristoylated) subunit. Studies of recoverin, a recently discovered myristoylated EF-hand protein, show that Ca^{2+} binding is not affected by the presence of the myristoyl group (Zozula & Stryer, 1992).

Energy Transfer: Inter-Metal Ion Distance Measurements. Förster-type energy transfer has been used to measure organic fluorophore–transition metal ion (Latt et al., 1972), intrinsic fluorophore–lanthanide ion (Horrocks & Collier, 1981), lanthanide ion–transition metal ion (Horrocks et al., 1975; Meares & Ledbetter, 1977), and inter-lanthanide ion (Mulqueen et al., 1985; Horrocks & Tingey, 1988; Wang et al., 1982; Snyder et al., 1981; Rhee et al., 1981) distances in proteins. In order to achieve this in CaM, where sites I and II bind with nearly equal affinities, Horrocks and Tingey used a 1:19 Eu^{3+}:Nd^{3+} metal ion mixture to avoid the presence of two Eu^{3+} ions in any one EF-hand pair (that is, to ensure that nearly every Eu^{3+} ion in the protein has a Nd^{3+} ion in the neighboring site). Due to the difference in affinities between the carboxyl-terminal CaN-B sites, the measurement is simplified: it is possible to fill site III with Eu^{3+} and then fill site IV with Nd^{3+}. This allows a good luminescence signal with minimal donor–donor pairings.

The Förster theory of energy transfer (Förster, 1948) states that the efficiency of energy transfer between a donor and an acceptor is dependent upon the distance between the two chromophores, the relative orientation of their transition dipoles, and their "spectral overlap". The efficiency of energy transfer, E, is given by

$$E = 1 - (\tau_{da}/\tau_d) \quad (2)$$

where τ_d is the lifetime of the donor ion in the absence of an acceptor and τ_{da} is the lifetime in the presence of acceptor. E is related to the inter-metal ion distance, r, by

$$r = R_0 [(1 - E)/E]^{1/6} \quad (3)$$

where R_0 is the critical distance for 50% energy transfer, given by the following equation:

$$R_0 = (8.78 \times 10^{-25})\kappa^2 \phi n^{-4} \quad (4)$$

Here κ^2 is the orientation factor, n is the refractive index of

the solvent, ϕ is the quantum yield of the donor, and J is the spectral overlap integral. The value of J is calculated via the following equation:

$$J = \int F(\nu)\epsilon(\nu)\nu^{-4}\,d\nu / \int F(\nu)\,d\nu \quad (5)$$

where $F(\nu)$ is the luminescence of the donor and $\epsilon(\nu)$ is the molar absorptivity of the acceptor at the frequency ν. κ^2 is taken to be $^2/_3$, the value for the isotropic case. A J value of 1.4×10^{-17} cm^{-6} mol^{-1}, determined by Horrocks and Tingey (1988) for Eu^{3+} and Nd^{3+} in CaM, was used in the calculations. The similarity between the Eu^{3+} excitation spectra of CaM and CaN-B makes it likely that their J values are close in magnitude.

Estimation of the quantum yield, ϕ, presents a problem. Often the ratio of the excited-state lifetimes in H_2O and D_2O, which is equal to the ratio of the quantum yields, is used as an estimate of ϕ_{H_2O}. For CaN-B, $\phi_{H_2O} = \tau(H_2O)/\tau(D_2O) = 0.52/2.17 = 0.24$. This estimate is only an upper limit, based on the assumption that $\phi_{D_2O} = 1$ (which is rarely the case). The quantum yield of Eu^{3+}(aq) in D_2O has been reported as 0.78 (Haas & Stein, 1971). In our calculations, we used $\phi_{D_2O} = 0.8$ since, due to the rather long lifetime of Eu^{3+}CaN-B in D_2O, it is reasonable to assume that nonradiative decay is at a minimum. In order to determine ϕ in H_2O/D_2O mixtures, the ratio of the lifetimes is multiplied by 0.8 to obtain the corrected quantum yield. Thus, for example, in 86% D_2O a quantum yield of $1.37/2.13 \times 0.8 = 0.51$ is obtained; likewise, in 97% D_2O, $\phi = 0.67$. With the above parameters, R_0 values of 10.9 and 10.4 Å are computed for the 97% and 86% D_2O solutions, respectively.

The distance between sites III and IV in CaN-B was measured by observing the luminescent decays of 1–5 μM solutions of this protein with Eu^{3+} (0.2–0.7 equiv) either alone or with Nd^{3+} added (2.0 equiv of total metal). In the presence of Nd^{3+}, two Eu^{3+} lifetimes are observed. In addition to the normal lifetime (1.79 ms in 97% D_2O) corresponding to the few EF-hand pairs with Eu^{3+} ions in both metal ion-binding sites, a shorter lifetime of 0.82 ms is observed. This lifetime corresponds to an inter-metal ion distance of 10.6 ± 0.5 Å. In 86% D_2O, lifetimes of 1.37 (unquenched) and 0.66 ms (quenched) yield a similar value of 10.4 ± 0.5 Å. The average estimated distance of 10.5 ± 0.5 Å is somewhat shorter than that of sites III and IV in CaM (11.5 Å; Babu et al., 1988), but is still within the range of distances found in EF-hand pairs. Recently acquired NMR structural data (Anglister et al., 1994) also indicate that the Ca^{2+}-binding loops of CaN-B are are arranged in EF-hand pairs, similar to CaM. The similarity of the CaM and CaN-B distances provides yet another example of the importance of the EF-hand motif to Ca^{2+}-binding function.

The possibility that the donor ion in site III or IV is quenched by an acceptor ion in site I or II is small; as in CaM and TnC, these sites are probably too far away to have any effect. It is reasonable to assume that CaN-B also possesses the long central helix that, when in an extended conformation, would cause an overall length of about 60 Å (Babu et al., 1988; Strynadka & James, 1989) and an interlobe, inter-metal ion distance of as much as 40 Å. Furthermore, there is much less sensitized emission of Tb^{3+} in the N-terminal lobe of CaN-B than CaM, militating against the possibility that CaN-B is a globular (spherical) rather than dumbbell-shaped protein.

The results presented here demonstrate that the overall structure of CaN-B is similar to those of the dumbbell-shaped proteins CaM and TnC; additionally, CaN-B is more like TnC than CaM in its binding of both lanthanide ions and Ca^{2+} and Mg^{2+}.

ACKNOWLEDGMENT

We thank Drs. JoAnne Bruno and Steven T. Frey for helpful discussions.

REFERENCES

Aitken, A., Cohen, P., Santikarn, S., Williams, D. H., Calder, A. G., Smith, A., & Klee, C. B. (1982) *FEBS Lett. 150*, 314–317.
Aitken, A., Klee, C. B., & Cohen, P. (1984) *Eur. J. Biochem. 139*, 663–671.
Albin, M., & Horrocks, W. D., Jr. (1985) *Inorg. Chem. 24*, 895–900.
Anglister, J., Grzesiek, S., Wang, A. C., Ren, H., Klee, C. B., & Bax, A. (1994) *Biochemistry 33*, 3540–3547.
Babu, Y. S., Bugg, C. E., & Cook, W. J. (1988) *J. Mol. Biol. 254*, 191–204.
Brittain, H. G., Richardson, F. S., & Martin, R. B. (1976) *J. Am. Chem. Soc. 98*, 8255–8260.
Bruno, J., Horrocks, W. D., Jr., & Zauhar, R. J. (1992) *Biochemistry 31*, 7016–7026.
Collins, J. H. (1974) *Biochem. Biophys. Res. Commun. 58*, 301–308.
Eads, C. D., Mulqueen, P., Horrocks, W. D., Jr., & Villafranca, J. J. (1985) *Biochemistry 24*, 1221–1226.
Förster, T. (1948) *Ann. Phys. 2*, 55–75.
Fritz, J. S., Oliver, R. T., & Pietrzyk, D. J. (1958) *Anal. Chem. 30*, 1111–1114.
Fruman, D. A., Klee, C. B., Bierer, B. E., & Burakoff, S. J. (1992) *Proc. Natl. Acad. Sci. U.S.A. 89*, 3686–3690.
Goldstein, R. F., & Leung, E. (1990) *Anal. Biochem. 190*, 220–232.
Grand, R. J. A., & Perry, S. V. (1978) *FEBS Lett. 92*, 137–142.
Guerini, D., Krinks, M. H., Sikela, J. M., Hahn, W. H., & Klee, C. B. (1989) *DNA 8*, 675–682.
Haas, Y., & Stein, G. (1971) *J. Phys. Chem. 75*, 3668–3677.
Hashimoto, Y., Perrino, B. A., & Soderling, T. R. (1990) *J. Biol. Chem. 265*, 1924–1927.
Henzl, M. T., McCubbin, W. D., Kay, C. M., & Birnbaum, E. R. (1985) *J. Biol. Chem. 260*, 8447–8455.
Herzberg, O., & James, M. N. G. (1988) *J. Mol. Biol. 203*, 761–779.
Horrocks, W. D., Jr. (1993) *Methods Enzymol. 226*, 495–538.
Horrocks, W. D., Jr., & Sudnick, D. R. (1979) *J. Am. Chem. Soc. 101*, 334–340.
Horrocks, W. D., Jr., & Collier, W. E. (1981) *J. Am. Chem. Soc. 103*, 2856–2862.
Horrocks, W. D., Jr., & Sudnick, D. R. (1981) *Acc. Chem. Res. 14*, 384–392.
Horrocks, W. D., Jr., & Tingey, J. M. (1988) *Biochemistry 27*, 413–419.
Horrocks, W. D., Jr., Holmquist, B., & Vallee, B. L. (1975) *Biochemistry 72*, 4764–4768.
Hubbard, M. J., & Klee, C. B. (1989) *Biochemistry 28*, 1868–1874.
Jahnke, U., & Heilmeyer, L. M. G., Jr. (1980) *Eur. J. Biochem. 111*, 325–332.
Kilhoffer, M. C., Demaille, J. G., & Gerard, D. (1980) *FEBS Lett. 116*, 269–272.
Kincaid, R. L., Nightingale, M. S., & Martin, B. M. (1988) *Proc. Natl. Acad. Sci. U.S.A. 85*, 8983–8987.
King, M. M., & Huang, C. Y. (1983) *Biochem. Biophys. Res. Commun. 114*, 955–961.
King, M. M., & Huang, C. Y. (1984) *J. Biol. Chem. 259*, 8847–8856.
Klee, C. B., & Krinks, M. H. (1978) *Biochemistry 17*, 120–126.
Klee, C. B., Crouch, T. H., & Krinks, M. H. (1979) *Proc. Natl. Acad. Sci. U.S.A. 76*, 6270–6273.

Klee, C. B., Krinks, M. H., Manalan, A. S., Cohen, P., & Stewart, A. A. (1983) *Methods Enzymol. 102*, 227–244.
Klee, C. B., Krinks, M. H., Manalan, A. S., Draetta, G. F., & Newton, D. L. (1985) in *Advances in Protein Phosphatases 1* (Merleverde, W., & DiSalvo, J., Eds.) pp 135–146, Leuven University Press, Leuven, Belgium.
Klee, C. B., Draetta, G. F., & Hubbard, M. J. (1987) *Adv. Enzymol. 61*, 149–200.
Kretsinger, R. H. (1973) *Adv. Cycl. Nucleotide Res. 11*, 2–26.
Latt, S. A., Auld, D. S., & Vallee, B. L. (1972) *Biochemistry 11*, 3015–3022.
Leavis, P. C., Nagy, B., Lehrer, S. S., Bialkowska, H., & Gergely, J. (1980) *Arch. Biochem. Biophys. 200*, 17–21.
Li, W., & Handschumacher, R. E. (1993) *J. Biol. Chem. 268*, 14040–14044.
Liu, J., Farmer, J. D., Jr., Lane, W. S., Freidman, J., Weissman, I., & Schreiber, S. L. (1991) *Cell 66*, 807–815.
Marsden, B. J., Shaw, G. S., & Sykes, B. D. (1990) *Biochem. Cell Biol. 68*, 587–601.
McNemar, C. W., & Horrocks, W. D., Jr. (1989) *Appl. Spectrosc. 43*, 816–821.
McNemar, C. W., & Horrocks, W. D., Jr. (1990) *Biochim. Biophys. Acta 1040*, 229–236.
Meares, C. F., & Ledbetter, J. E. (1977) *Biochemistry 16*, 5178–5180.
Merat, D. L., & Cheung, W. Y. (1993) *FASEB J. 7*, A1158.
Merat, D. L., Hu, Z. Y., Carter, T. E., & Cheung, W. Y. (1985) *J. Biol. Chem. 260*, 11053–11059.
Minowa, O., & Yagi, K. (1984) *J. Biochem. (Tokyo) 96*, 1175–1182.
Mulqueen, P., Tingey, J. M., & Horrocks, W. D., Jr. (1985) *Biochemistry 24*, 6639–6645.
Politino, M., & King, M. M. (1987) *J. Biol. Chem. 262*, 10109–10113.
Rao, J., & Wang, J. H. (1989) *J. Biol. Chem. 264*, 1058–1061.
Rhee, M.-J., Sudnick, D. R., Arkle, V. K., & Horrocks, W. D., Jr. (1981) *Biochemistry 20*, 3328–3333.
Sambrook, J., Fritsch, E. F., & Maniatis, T. (1989) *Molecular Cloning: A Laboratory Manual*, 2nd ed. (Nolan, C., Ed.) Cold Spring Harbor Laboratory Press, Cold Spring Harbor, NY.
Shannon, R. D. (1976) *Acta Crystallogr., Sect. A 32*, 751–767.
Sharma, R. K., Desai, R., Waisman, D. M., & Wang, J. H. (1979) *J. Biol. Chem. 254*, 4276–4282.
Shatzman, A. R., & Rosenberg, M. (1987) *Methods Enzymol. 152*, 661–673.
Snyder, A. P., Sudnick, D. R., Arkle, V. K., & Horrocks, W. D., Jr. (1981) *Biochemistry 20*, 3334–3339.
Stewart, A. A., Ingebritsen, T. S., Manalan, A., Klee, C. B., & Cohen, P. (1982) *FEBS Lett. 137*, 80–84.
Studier, F. W., Rosenberg, A. H., Dunn, J. J., & Dubendorf, J. W. (1990) *Methods Enzymol. 185*, 60–89.
Styrnadka, N. C. J., & James, M. N. G. (1989) *Annu. Rev. Biochem. 58*, 951–998.
Towler, D. A., Gordon, J. I., Adams, S. P., & Galser, L. (1989) *Annu. Rev. Biochem. 57*, 69–99.
Ueki, K., Muramatsu, T., & Kincaid, R. L. (1993) *FASEB J. 7*, A1158.
Wang, C.-L., Leavis, P. C., Horrocks, W. D., Jr., & Gergely, J. (1981) *Biochemistry 20*, 2439–2444.
Wang, C.-L. A., Tao, T., & Gergely, J. (1982) *J. Biol. Chem. 257*, 8372–8375.
Wang, C.-L. A., Leavis, P. C., & Gergely, J. (1984) *Biochemistry 23*, 6410–6415.
Winkler, M. A., Merat, D. L., Tallant, E. A., Hawkins, S., & Cheung, W. Y. (1984) *Proc. Natl. Acad. Sci. U.S.A. 81*, 3054–3058.
Zozula, S., & Stryer, L. (1992) *Proc. Natl. Acad. Sci. U.S.A. 89*, 11569–11573.